Hybrid Beamforming Using Convex Optimization for SDMA in Millimeter Wave Radio

Sau-Hsuan Wu, Ko-Yen Lin, and Lin-Kai Chiu
Department of Communication Engineering
National Chiao Tung University, Hsinchu, Taiwan
E-mail:{sauhsuan@cm.nctu.edu.tw, linkillua.cm96g@g2.nctu.edu.tw, sazabi.cm94g@nctu.edu.tw}

Abstract— **A radio-frequency and baseband hybrid beamforming (HBF) scheme is presented for spatial division multiple access (SDMA) of 60GHz applications using planar antenna arrays (PAA). PAA with phase shifters for each element antenna is partitioned into sub-blocks and each block is applied a common baseband beamforming weight. To suppress the grating lobes of beam pattern and to maintain the signal to interference plus noise ratio (SINR) of users in the SDMA system, we study the design of this HBF using convex optimization. Two design criteria are considered herein: one minimizes the transmit power subject to a SINR constraint, and the other maximizes the worst case SINR subject to a total power constraint. Simulation results show that both the SINR and directivity of HBF can be significantly improved by making use of the convex optimization technique.**

Keywords— **Planar antenna arrays, hybrid beamforming, SDMA, convex optimization and 60GHz millimeter wave.**

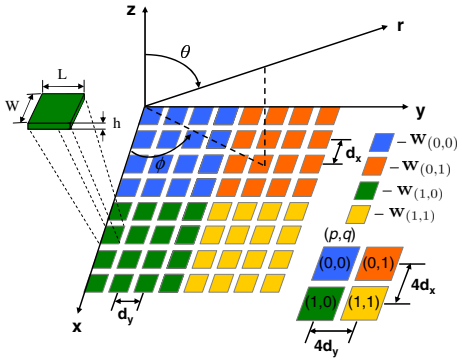

Fig. 1. Antenna arrays of 8×8 planar antennas. Patch antennas in different colors belong to different blocks.

I. Introduction

The increasing demands on bandwidth for personal and indoor wireless multimedia applications have driven the research and development for a new generation of broadband wireless personal area network (WPAN) [1]. The characteristics of broad unlicensed bandwidth, high penetration loss and significant oxygen absorption [2] at 60GHz radio make it an ideal wireless interface for the next generation WPAN. Furthermore, the millimeter wavelength of 60GHz makes it feasible to use tens of tiny antennas to steer radio signals with high directivity to increase wireless link qualities and spatial reuse factors. In view of the advantages of beamforming (BF) for 60GHz radio, we present herein a cost-effective hybrid BF (HBF) technique for spatial division multiple access (SDMA) using planar antenna arrays (PAA).

Digital BF has been used to compensate the rather fixed radiation patterns of switch-beam or beam-selection antennas to synthesize more flexible hybrid beam patterns [3]. In conjunction with the phase shifters of the element patch antennas of PAA, a hybrid type of digital and RF BF (HBF) is studied in [4]. Motivated by the above results and taking into account the practical limitation and implementation costs of the full digital BF, we study herein a special type of HBF for two-user SDMA using a 8×8 PAA as illustrated in Fig. 1. The entire PAA is partitioned into four blocks of patch antennas. Each block is driven by a digital BF weight, while each element patch antenna in a block is equipped with an individual phase shifter. To suppress the grating lobes resulting from the over-reduced number of digital BF weights [5], and to maintain the quality of service (QoS) for users in the SDMA system, we study the design of this HBF from the perspective of convex optimization.

This research has been funded in part by the NCTU MTK Research Center, Taiwan, and in part by the National Science Council, Taiwan, under Grant NSC 97-2219-E-009-004.

Convex optimization has found many applications in BF designs, *e.g.* [6, 7]. Of which, [7] uses BF to compensate the effects of wireless channels at the transmitter side. Motivated by this transmit BF method, we employ two design criteria herein for the HBF of SDMA based on convex optimization: the maximization of the interference plus noise ratios (SINRs) for users in the system subject to a total power constraint on PAA, and the minimization of the total power consumption subject to a SINR constraint for users in the system. Simulation results show that both the SINR and directivity of HBF can be improved with the convex optimization techniques and are much higher than those obtained with conventional BF schemes such as the linear constrained minimum power method [8].

II. Hybrid beamforming for SDMA using PAAs

We specify the configuration of PAA for HBF at first. Sixty-four identical patch antennas are aligned to form an 8×8 antenna matrix as shown in Fig. 1. Each element antenna is equipped with a phase shifter to maneuver the phase of the signal radiating through it. Given the large number of antennas available for 60GHz applications, it is beneficial to use the antennas to serve multiple users (the concept of SDMA) in addition to increasing the received signal to noise ratio of a single user. However, adjusting only the phases of the radio signals sometimes may not be able to achieve the desired SINR for the user of interest, as the beam direction of the user might be severely jammed by the side beams of other users. To overcome this difficulty, baseband (BB) BF techniques can be used to jointly steer the beam patterns and suppress the interference for all users. Taking into account the practical limitations of circuit implementations, the arrays of antennas are partitioned into blocks,

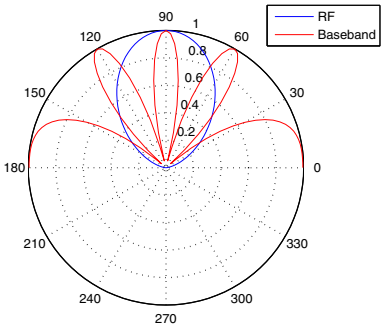

Fig. 2. Polar plot of the hybrid beamforming pattern with the configuration of PAA in Fig. 1 when $\theta = \pi/2$.

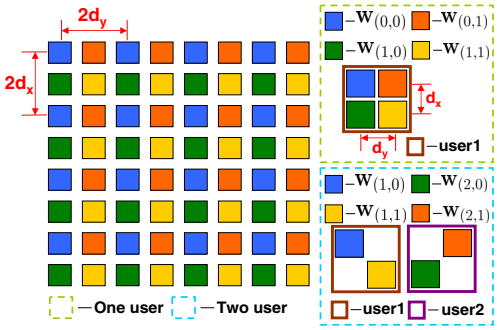

Fig. 3. Configurations of the rearranged planar antenna arrays for the applications of one-user and two-user HBFs.

and each of which is driven by a digital BF weight. Given the BF weights, the composite array pattern of HBF can be calculated with the standard antenna theory [5].

A. The composite array pattern of hybrid beamforming

To facilitate the analysis and highlight the performance of HBF, the coupling effects among element antennas are neglected in the sequel. As a result, the total beam pattern of a block of a partition can be expressed as the product of the electric field of a single antenna and the array factor corresponding to the block [5]. The far-zone electric field of a single element antenna is given by

$$E(\phi,\theta) = E_\theta \overrightarrow{a_\theta} + E_\phi \overrightarrow{a_\phi} + E_r \overrightarrow{a_r}$$

where

$$E_\theta = j\frac{hWkE_0e^{-jkr}}{\pi r}\left[\cos\phi\cos X\left(\frac{\sin Y}{Y}\right)\left(\frac{\sin Z}{Z}\right)\right]$$

$$E_\phi = j\frac{hWkE_0e^{-jkr}}{\pi r}\left[\cos\theta\sin\phi\cos X\left(\frac{\sin Y}{Y}\right)\left(\frac{\sin Z}{Z}\right)\right]$$

and $E_r \cong 0$ as $r \gg \frac{2LW}{\lambda}$ (see [5] for the far field definition). The physical meaning of some parameters are illustrated in Fig. 1, and E_0 is a constant. For convenience of expression, we also define $X \triangleq \frac{kL}{2}\sin\theta\cos\phi$, $Y \triangleq \frac{kW}{2}\sin\theta\sin\phi$, $Z \triangleq \frac{kh}{2}\cos\theta$ and $k \triangleq \frac{2\pi}{\lambda}$ with λ being the radio wavelength.

Now define an index pair, $(p,\ q) \in \{0,1\}^2$, for each block of the PAA in Fig. 1. Given the index pair $(p,\ q)$ of a block, the corresponding array factor follows

$$A_{(p,q)}(\phi,\theta) = e^{jpN\left(\Psi_x+\beta_{x,(p,q)}\right)}\sum_{n=1}^{N} e^{j(n-1)(\Psi_x+(-1)^p\beta_{x,(p,q)})} \times e^{jqM\left(\Psi_y+\beta_{y,(p,q)}\right)}\sum_{m=1}^{M} e^{j(m-1)(\Psi_y+(-1)^q\beta_{y,(p,q)})}$$

where $\Psi_x \triangleq kd_x\cos\phi\sin\theta$ and $\Psi_y \triangleq kd_y\sin\phi\sin\theta$. The physical meaning of the parameters can also be found in Fig. 1. Besides, $\beta_{x,(p,q)}$ and $\beta_{y,(p,q)}$ are the corresponding phase differences in the x and y directions between adjacent patch antennas (see the definitions in [9]). The number of antennas in the x direction of a block is N and the number of antennas in the y direction is M.

To distinguish the array factor $B(\phi,\theta)$ formed with the BB BF weights of a user from the array factor $A(\phi,\theta)$ obtained by tuning the phase of the radiated wave of each antenna, we refer to $B(\phi,\theta)$ as the baseband array factor (BAF) in contrast to the array factor $A(\phi,\theta)$ tuned in the RF band.

Now we consider this hybrid type of baseband and RF BF for the simple partition shown in Fig. 1. Suppose that the RF array factor (RAF) for different blocks of a user are the same and pointed to the desired direction of interest, the composite beam pattern of HBF is given by

$$H(\phi,\theta) \triangleq B(\phi,\theta)A(\phi,\theta)E(\phi,\theta) \tag{1}$$

where $A(\phi,\theta)$ is the array factor of the 4×4 antenna arrays. In the extreme case of Fig. 1 that the entire PAA is used to support a single user, the BAF is given by

$$B(\phi,\theta) = \sum_{r=0}^{1}\sum_{s=0}^{1} w_{(r,s)}e^{j4r\Psi_x}e^{j4s\Psi_y}. \tag{2}$$

where $\Psi_x \triangleq kd_x\cos\phi\sin\theta$ and $\Psi_y \triangleq kd_y\sin\phi\sin\theta$. The enlarged distances between the adjacent effective antennas make $4kd_x = 4kd_y = 4\pi$ in (2) as $dx = dy = \lambda/2$, which in turn results in the periodic BB beam pattern of $B(\phi,\theta)$ shown in Fig. 2. The angular coordinate corresponds to the elevation angle θ and the radial coordinate shows the normalized BF gain. Due to the periodic pattern, the product of $B(\phi,\theta)$ and $A(\phi,\theta)$ will yield significant sidelobes on both sides of the main beam. For clarity, the RAF $A(\phi,\theta)$ of the 4×4 block is also shown in the figure. Since the patch antenna has a fixed radiation pattern, its pattern is not shown in the figure.

The strong sidelobes of HBF with the partition in Fig. 2 will cause sever interference in SDMA. To suppress the sidelobe while still be able to benefit from the advantage of HBF, we consider an alternative partition in Fig. 3. Patch antennas of the same color belong to a block and are driven by the same BB BF weights. Thus, the PAA is still partitioned into four blocks in Fig. 3. With this partition, the distances between two element antennas increase to $(2d_x, 2d_y)$ in both the x and y axes. While the largest distances between any two effective antennas become $(d_x,\ d_y)$ of the distances between the blue and the yellow blocks. Consequently, the periodicity will now appear in the RAF in stead of the BAF.

Fig. 4 shows the polar plots of the BAF and RAF according to the partition in Fig 3 when $\theta_d = \pi/2$. The RAF still bears the same form except that the parameters d_x and d_y now become $2d_x$ and $2d_y$, respectively. On the other hand, the BAF now becomes the form of

$$B(\phi,\theta) = \sum_{r=0}^{1}\sum_{s=0}^{1} w_{(r,s)}e^{jr\Psi_x}e^{js\Psi_y}. \tag{3}$$

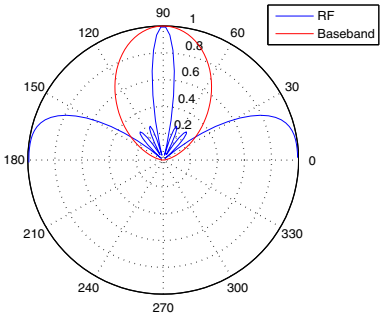

Fig. 4. Polar plot of the hybrid beamforming pattern with the rearranged PAA in Fig. 3 when $\theta = \pi/2$.

Despite the periodic pattern of RAF, it clearly shows that the product of $B(\phi,\theta)$ and $A(\phi,\theta)$ will form a sharper and stronger mainbeam along the desired direction. This makes the configuration in Fig. 4 more suitable for joint beam steering and interference suppression in SDMA.

According to the configuration of Fig. 3, we consider a partition to implement the HBF for two-user SDMA. The antennas in blue and yellow colors of Fig. 3 belong to user one, and the antennas in green and orange belong to user two. That is two BF weights are employed for each user. The resultant BAF for user one and two are given by

$$B_1(\phi,\theta) = w_{(1,0)} + w_{(1,1)}e^{j\Psi_x + j\Psi_y} = w_1^H \mathbf{s}_1(\phi,\theta) \quad (4)$$

$$B_2(\phi,\theta) = w_{(2,0)}e^{j\Psi_x} + w_{(2,1)}e^{j\Psi_y} = w_2^H \mathbf{s}_2(\phi,\theta) \quad (5)$$

where w_i^H is the weight vector for user i. The steering vectors of user 1 and 2 in (4) and (5) can be shown as followings

$$\mathbf{s}_1(\phi,\theta) \triangleq [1 \quad e^{j(\Psi_x+\Psi_y)}]^T \quad (6)$$

$$\mathbf{s}_2(\phi,\theta) \triangleq [e^{j\Psi_x} \quad e^{j\Psi_y}]^T. \quad (7)$$

Now to steer the main beam towards the direction of the user of interest and, in the mean time, to suppress the interference in the direction of the other user, a typical method is the so-called maximum directivity (MD) BF [10]. Though simple and straightforward, the MD BF does not offer the degrees of freedom to control the total power of BF and more, importantly, the SINR in SDMA. In the next section, we refine the design of HBF making use of the concept of convex optimization.

III. Multiuser hybrid beamforming based on convex optimization

Our goals for the design of HBF for SDMA are twofold: one is to minimize the overall power consumption subject to (*s.t.*) the signal quality constraint of each user, the other is to look for the best SINR for each user subject to the total power constraint. To meet the design objectives, we consider a number of design criteria from the perspective of convex optimization. They are classified into two categories and described in the following subsections.

A. HBF based on the constrained minimization of power

A widely used approach for power minimization is the linear constrained minimum power (LCMP) method [8], which minimizes the power of BF and, in the mean time, nulls the interference in the beam direction of the user of interest. Therefore, we first study LCMP for the HBF of SDMA.

A.1 Power minimization based on LCMP

Let $u_i(t), i \in \{1,2\}$ be the transmitted signal of user i, with $E[|u_i(t)|^2] = 1$. The baseband transmitted signal for the two-user SDMA can be modeled as

$$\mathbf{x}(t) = \mathbf{s}_1 u_1(t) + \mathbf{s}_2 u_2(t). \quad (8)$$

where the steering vectors $\mathbf{s}_1$ and $\mathbf{s}_2$ are defined in (6) and (7), respectively. To design the BF weight vector $\mathbf{w}_i$ for user i such that the output power and the interference to the beam direction of the other user are both minimized, the LCMP is formulated as

$$\begin{array}{ll} \arg\min_{\mathbf{w}_i} & \mathbf{w}_i^H \mathbf{S}_x \mathbf{w}_i \\ \text{s.t.} & \mathbf{w}_i^H \mathbf{C} = \mathbf{e}_i \end{array}$$

where $\mathbf{S}_x \triangleq E\{\mathbf{x}^2(t)\}$, $\mathbf{C} \triangleq [\mathbf{s}_i(\phi_1,\theta_1), \mathbf{s}_i(\phi_2,\theta_2)]$ with $\{\phi_i,\ \theta_i\}$ being the desired beam direction of user i, and $\mathbf{e}_i$ is a 1×2 basis vector with 1 in the ith position and the other zero. The above optimization problem can be easily solved by making use of the Lagrange multiplier as below

$$J = \mathbf{w}_i^H \mathbf{S}_x \mathbf{w}_i + \left[\mathbf{w}_i^H \mathbf{C} - \mathbf{e}_i^H\right] \lambda + \lambda^H \left[\mathbf{C}^H \mathbf{w}_i - \mathbf{e}_i\right] \quad (9)$$

with $\lambda \triangleq [\lambda_1, \lambda_2]^T$. The resultant optimal BF weight vector for user i is given by

$$\mathbf{w}_i^H = \mathbf{e}_i^H [\mathbf{C}^H \mathbf{S}_x^{-1} \mathbf{C}]^{-1} \mathbf{C}^H \mathbf{S}_x^{-1}. \quad (10)$$

A.2 Power minimization based on SOCP

The BF weight vectors obtained with the LCMP method are essentially carried out individually. The output powers for user one and two are not jointly minimized. In addition, we often are more interested in searching for BF weights that can guarantee the SINR for each user. To design BF weights that fulfill the above goals, we adopt an alternative approach making use of the standard second order cone programming (SOCP) for convex optimization problem.

To formulate the design for BF weights that minimize the power consumption and maintain the SINR, we first define the SINR for SDMA using HBF. For convenience of expression, we rewrite the composite beam pattern (1) for user i as

$$\begin{aligned} H_i(\phi,\theta) &= \mathbf{w}_i^H \mathbf{s}_i(\phi,\theta) A_i(\phi,\theta) E(\phi,\theta) \\ &= \mathbf{w}_i^H \mathbf{g}_i(\phi,\theta),\ i \in \{1,2\}. \end{aligned}$$

Following the above notations, the SINR with respect to the i-th user at its desired beam direction (ϕ_i,θ_i) is defined as

$$\text{SINR}_i(\phi_i,\theta_i) = \frac{\|\mathbf{w}_i^H \mathbf{g}_i(\phi_i,\theta_i)\|^2}{\Sigma_{j\neq i}\|\mathbf{w}_j^H \mathbf{g}_j(\phi_i,\theta_i)\|^2 + \sigma_n^2}, \quad (11)$$

where σ_n^2 is the noise variance. Given the SINR definition, now minimizing the total baseband power subject to SINR constraints can be formulated as

$$\mathcal{P}(\gamma_0) = \left\{ \begin{array}{ll} \arg\min_{\mathbf{w}_i} & \sum_{i=1}^2 \|\mathbf{w}_i\|^2 \\ \text{s.t.} & \min_i \text{SINR}_i(\phi_i,\theta_i) \geq \gamma_0 \\ & i \in \{1,2\} \end{array} \right. \quad (12)$$

where $\gamma_0 > 0$ is the lower bound on the SINR.

This above strategy guarantees that all users can at least receive a QoS characterized by γ_0. Since the BF vector with an arbitrary phase rotation is still optimal as long as the BF vector itself is already optimal. Without the loss of generality, we can constrain $\mathbf{w}_i^H \mathbf{g}_i$ to be nonnegative real. Define

$$\mathbf{G}(\phi_i, \theta_i) = \begin{bmatrix} \mathbf{g}_1(\phi_i, \theta_i) & \mathbf{0} \\ \mathbf{0} & \mathbf{g}_2(\phi_i, \theta_i) \end{bmatrix} \tag{13}$$

which is a matrix of dimension 4×2 and let $\widetilde{\mathbf{w}} = \text{vec}\{\mathbf{w}_1, \mathbf{w}_2\}$ where vec(.) is the vectorization operation. By the results in [7], the optimization problem now becomes

$$\mathcal{P}(\gamma_0) = \begin{cases} \min_{\{\mathbf{w}_i, p\}} & p \\ \text{s.t.} & \sqrt{1+\frac{1}{\gamma_0}}\ \mathbf{w}_i^H \mathbf{g}_i \geq \left\| \begin{array}{c} \mathbf{G}^H(\phi_i, \theta_i)\widetilde{\mathbf{w}} \\ \sigma_n \end{array} \right\| \\ & \|\widetilde{\mathbf{w}}\| \leq \sqrt{p} \end{cases} \tag{14}$$

which is of the standard form of SOCP, thus can be solved efficiently by using the CVX toolbox [11].

B. HBF based on the constrained maximization of SINR

Another strategy for HBF design is to maximize the minimal SINR among all users subject to a constraint on the sum of all users' transmitted power. The design problem is formulated as

$$\mathcal{S}(P_0) = \begin{cases} \max_{\{\mathbf{w}_i\}} & \min_i \text{SINR}_i(\phi_i, \theta_i) \\ \text{s.t.} & \sum_{i=1}^2 \|\mathbf{w}_i\|^2 \leq P_0 \end{cases} \tag{15}$$

where $P_0 > 0$ is the upper bound on the total sum power.

Unfortunately, (15) can not be formulated as a convex optimization problem. Nevertheless, it can be solved with an iterative algorithm in [7] that makes use of the connection between power minimization and SINR maximization. The iterative procedure is based on the following theorem [7].

Theorem 1: [7] The power minimization problem of (12) and the SINR maximization problem of (15) are inverse problems, namely

$$\gamma_0 = \mathcal{S}(\mathcal{P}(\gamma_0))$$
$$P_0 = \mathcal{P}(\mathcal{S}(P_0)).$$

Furthermore, the optimal objective value of each optimization problem is continuous, and is strictly and monotonically increasing with its input argument, *i.e.*

$$\gamma_0 > \tilde{\gamma_0} \Longrightarrow \mathcal{P}(\gamma_0) > \mathcal{P}(\tilde{\gamma_0})$$
$$P_0 > \tilde{P_0} \Longrightarrow \mathcal{S}(P_0) > \mathcal{S}(\tilde{P_0}).$$

The proof of this theorem can be found in [7]. Based on Theorem 1, $\mathcal{S}(P_0)$ can be solved iteratively with the algorithm summarized below.

Algorithm 1

1: Initialize γ_{min} = MinSINR and γ_{max} = MaxSINR
2: repeat
3: $\quad \gamma_0 \longleftarrow (\gamma_{min} + \gamma_{max})/2$
4: $\quad \widehat{P}_0 \longleftarrow \mathcal{P}(\gamma_0)$
5: $\quad$ if $\widehat{P}_0 \leq P_0$
6: $\quad\quad$ then $\gamma_{min} \longleftarrow \gamma_0$
7: $\quad\quad$ else $\gamma_{max} \longleftarrow \gamma_0$
8: until $\widehat{P}_0 = P_0$
9: return γ_0 and $\mathbf{w}_i$

The MinSINR and MaxSINR must be adjusted such that $\widehat{P}_0 = P_0$ exists with a feasible $\gamma_0 \in [\text{MinSINR}, \text{MaxSINR}]$.

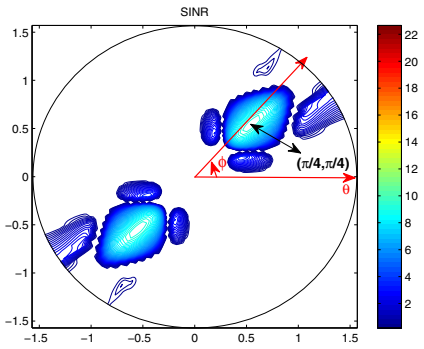

Fig. 5. The contour plot of SINR for user 1, using the RF beamforming, with the desired directions of user one and two set at (ϕ_1, θ_1)=$(\pi/4, \pi/4)$ and (ϕ_2, θ_2)=$(3\pi/4, \pi/4)$, respectively.

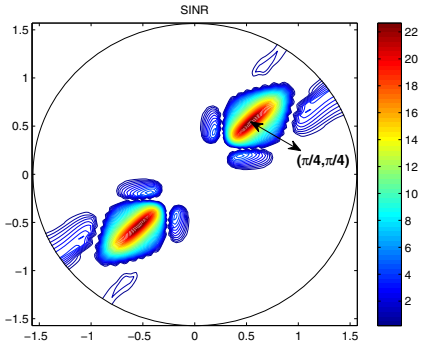

Fig. 6. The contour plot of SINR for user 1, using the HBF of LCMP, with the desired directions of user one and two set at (ϕ_1, θ_1)=$(\pi/4, \pi/4)$ and (ϕ_2, θ_2)=$(3\pi/4, \pi/4)$, respectively.

IV. Computer Simulations

We demonstrate simulation results for the HBF schemes proposed in the previous section for SDMA. The transmit signal to noise ratio in the following simulations is set to 30 dB for each user if no specific description.

Fig. 5 presents the contour plot of SINR for user 1 when using the RF BF method. The desired directions of user one and two are set at (ϕ_1, θ_1)=$(\pi/4, \pi/4)$ and (ϕ_2, θ_2)=$(3\pi/4, \pi/4)$, respectively. A similar SINR contour plot for user 1 is also shown in Fig. 6 when using the HBF of LCMP. The contour plots are shown in the cylindrical coordinate. The radial coordinate maps to the elevation angle θ and the angular coordinate maps to the azimuth angle ϕ. The value of $\text{SINR}_1(\phi_1, \theta_1)$ for user 1 in Fig. 5 is equal to 9.366 dB, while it is equal to 23.817 dB in Fig. 6 with the HBF of LCMP. This demonstrates that the interference can be effectively suppressed in the desired direction of user 1 using the HBF method.

In addition to SINR, directivity is also an important performance measure to characterize the effectiveness of BF. To reflect the interference due to the multiple access in SDMA, the original definition for directivity in [5] is modified into

$$D_i = \frac{\text{SINR}_i(\phi_i, \theta_i)}{\int_0^{2\pi} \int_0^{\frac{\pi}{2}} |H_i(\phi, \theta)|^2 \sin(\theta) d\theta d\phi}. \quad (dB) \tag{16}$$

This new definition for directivity automatically refers to the traditional notion of directivity in the single-user system.

User1 User2 (ϕ, θ)	User1 (π/8, π/4)				User2 (π/4, π/4)			
	RF	MD	LCMP	Opt.1	RF	MD	LCMP	Opt.1
SINR (dB)	20.94	6.993	6.993	22.84	22.43	18.87	18.87	22.84
Directivity	34.74	20.85	20.85	37.71	36.20	32.60	32.60	35.59
P_T	0.0417	0.0411	0.0411	0.0325	0.042	0.0423	0.0423	0.0531

Fig. 7. The SINRs, directivities and the radiation power of the RF BF and the HBF schemes of MD, LCMP and Opt. 1.

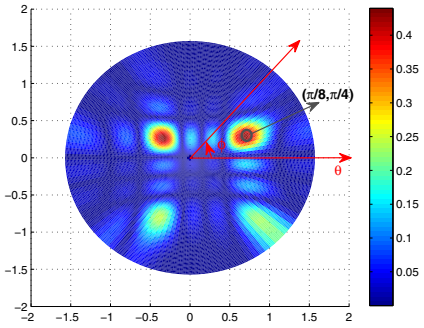

Fig. 8. The beam pattern of user 1 using the RF BF, with the desired direction in (ϕ_1, θ_1)=$(\pi/8, \pi/4)$.

Fig. 7 shows the simulation results for the SINR, directivity and the radiation power of various BF schemes for SDMA when the desired directions are set at $(\phi_1, \theta_1) = (\pi/8, \pi/4)$ and $(\phi_2, \theta_2) = (\pi/4, \pi/4)$. The Opt. 1 refers to the HBF scheme of (15) solved with Algorithm 1 in Section III-B. The radiation power for each user is evaluated with

$$\int_0^{2\pi} \int_0^{\frac{\pi}{2}} |H_i(\phi, \theta)|^2 \sin(\theta) d\theta d\phi, \qquad (17)$$

and is denoted by P_T in the figure.

In this case, even thought RF BF presents similar SINRs of the HBF of Opt. 1, the directivitiy for user 1 of Opt. 1 is much higher than that of the RF BF. However, the directivity for user 2 of Opt. 1 is lower than that of the RF BF. This phenomenon on directivity can be interpreted by users' beam patterns in Fig. 8 $\sim$ Fig. 10.

The beam pattern of user 1 when using the RF BF is presented in Fig. 8. On the other hand, the beam pattern

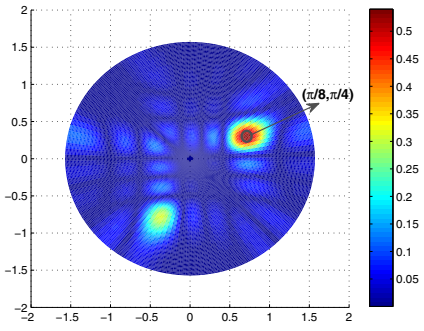

Fig. 9. The beam pattern of user 1 using the HBF of (15), with the desired direction in (ϕ_1, θ_1)=$(\pi/8, \pi/4)$.

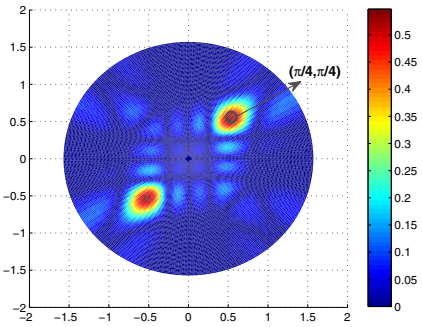

Fig. 10. The beam pattern of user 2 using the HBF of (15), with the desired direction in (ϕ_2, θ_2)=$(\pi/4, \pi/4)$.

of user 1 when using the HBF of (15) is shown in Fig. 9. Obviously, there are a strong sidelobe and other two weak ones in addition to the mainlobe in Fig. 8. However, there only exists a weak sidelobe in Fig. 9. This indicates that the power for user 1 is more concentrated to its desired direction with the HBF of (15), thus leading to a higher directivity for user 1 in Fig. 7.

The corresponding beam pattern of user 2 when using the HBF of (15) is also shown in Fig. 10. Compared with that of user 1 in Fig. 9, user 2 has an obvious sidelobe in $(\phi, \theta) = (5\pi/4, \pi/4)$, thus offering a lower directivity than user 1. Besides, directivities of user 2 with Opt.1 are lower than those of the RF BF. Actually, Fig. 7 shows the radiation power of user 2 with Opt.1 is higher than that of the RF BF, and the SINRs of them are close. It means user 2 must apply more radiation power to achieve the similar SINR of RF BF. Thus, by the definition of directivity in (16), user 2 with Opt.1 has smaller directivity than RF BF.

References

[1] "IEEE 802.15 WPAN Millimeter Wave Alternative PHY Task Group (TG3c)," available at http://www.ieee802.org/15/pub/TG3c.html.

[2] C. R. Anderson and T. S. Rappaport, "In-building wideband partition loss measurements at 2.5 and 60 GHz," *IEEE Trans. on Communications*, vol. 3, no. 3, pp. 922–928, May 2004.

[3] M. Rezk, W. Kim, Z. Yun, and M.F. Iskander, "Performance comparison of a novel hybrid smart antenna system versus the fully adaptive and switched beam antenna arrays," *IEEE Antennas and Wireless Propagation Letters*, vol. 4, pp. 285–288, Oct. 2005.

[4] A. B. Smolders and G. W. Kant, "THousand Element Array (THEA)," in *Proc. IEEE Antennas and Propagation Society International Symposium*. Salt Lake City, UT, July 2000.

[5] C. A. Balanis, *Antenna Theory*, John Wiley & Sons, 2 edition, 1997.

[6] Z.-Q. Luo and W. Yu, "An introduction to convex optimization for communications and signal processing," *IEEE Journal on Selected Areas in Communication*, pp. 1426–1438, Aug. 2006.

[7] A. Wiesel, Y. C. Eldar, and S.Shamai, "Linear precoding via conic optimization for fixed MIMO receivers," *IEEE Trans. on Signal Processing*, vol. 54, no. 1, pp. 161–176, Jan. 2006.

[8] H. L. Van Trees, *Optimum array processing. Part. IV of detection, estimation and modulation theory.*, John Wiley & Sons, 2002.

[9] S.-S. Wu, L.-K. Chiu, K.-Y. Lin, and S.-J. Chung, "Planar arrays hybrid beamforming for SDMA in millimeter wave applications," in *IEEE 19th PIMRC*. Cannes, France, 15-18 Sep. 2008.

[10] T. Kuhwald and H. Boche, "A constrained beam forming algorithm for 2D planar antenna arrays," in *Proc. IEEE VTC-Fall*. Amsterdam, The Netherlands, Sep. 1999.

[11] M. Grant and S. Boyd, "CVX: Matlab software for disciplined convex programming (web page and software)," Feb. 2009, http://stanford.edu/ boyd/cvx.